

Received March 14, 2021, accepted April 26, 2021, date of publication April 29, 2021, date of current version May 7, 2021.

Digital Object Identifier 10.1109/ACCESS.2021.3076533

Skin Lesion Classification by Multi-View Filtered Transfer Learning

JIANXIAO BIAN^{1,2}, SONG ZHANG³, SHAOQIANG WANG⁴,
JIANRUI ZHANG¹, AND JINCHANG GUO¹

¹School of Mechanical Engineering, Longdong University, Qingyang 745000, China

²Shaanxi Key Laboratory of Non-Traditional Machining, Xi'an Technological University, Xi'an 710021, China

³The Affiliated Hospital of Qingdao University, Qingdao 266000, China

⁴School of Computer and Communication Engineering, China University of Petroleum (East of China), Qingdao 266000, China

Corresponding authors: Jianxiao Bian (jxbian@ldxy.edu.cn) and Shaoqiang Wang (sqiang_wang@163.com)

This work was supported in part by the Open Research Fund Program of Shaanxi Key Laboratory of Non-Traditional Machining under Grant SXTZKFJJ201904, in part by the Doctoral Foundation Project of Longdong University under Grant XYBY1905, in part by the Science and Technology Program of Gansu Province under Grant 20JR5RA483, and in part by the Youth Science and Technology Fund of Gansu Province under Grant 21JR1RM340.

ABSTRACT Skin cancer is one of the most deadly cancer types with considerable number of patients. Image analysis has largely improved the automated diagnosis accuracy for malignant melanoma and other pigmented skin lesions, compared to unaided visual examination. Recent popular solution for automated skin lesion classification is using deep neural networks, trained from large amounts of professional annotated data, but that largely limits the model's scalability. This paper exploits transfer learning for skin lesion classification task with the help of labeled data from another domain (source), and proposes a multi-view filtered transfer learning network to strongly represent discriminative information from different image views with reasonable weighing strategy. This method also evaluates the importance for each source images, which can learn useful knowledge with neglecting negative samples from source domain. The extensive skin lesion classification experiments demonstrate our method can effectively solve Melanoma and Seborrheic Keratosis classification tasks with outstanding extensibility, and the discussion of the major components also testifies the improvements of our proposed multi-view filtered transfer learning approach.


INDEX TERMS Skin lesion classification, transfer learning, multi-view, filtered domain adaptation.

I. INTRODUCTION

Skin cancer expresses its severe harm to human health, where the malignancy leads to high fatality rate with frequently diagnosed around the world [1]. One of the most complicated types is malignant melanoma with considerable mortality rates. Taken American as example, current estimates are that one in five Americans will develop skin cancer in their lifetime, and it is estimated that approximately 9,500 people in the U.S. are diagnosed with skin cancer everyday [2]–[4]. Besides, research estimates that non-melanoma skin cancer (NMSC), including basal cell carcinoma (BCC) and squamous cell carcinoma (SCC), affects more than 3 million Americans per year, and the overall incidence of BCC increased by 145% between 1976-1984 and 2000-2010, while the overall incidence of SCC increased 263% over that same period [2], [5]. The major risk factor

of skin cancer for all types of melanoma and deadliest form is the exposure to natural/artificial ultraviolet light [3], and the detection of skin cancer can be implemented by dermatologists with observing skin changes in size, shape, or color of a mole or other skin lesion, the appearance of a new growth on the skin, or a sore that doesn't heal.

According to morphological signs mentioned above, the expertized skin cancer recognition requires intricate knowledge training in long-term period. However, several early symptoms are unobvious to confuse clinical examiner because of different training levels among dermatologists. To handle this intractable issue and release the labor-expensive workload, automated image recognition technology is integrated into intelligent skin lesion diagnosis [6]–[8] with the development of deep learning. Representatively, Pereira *et al.* [6] exploited the border-line characteristics of the lesion segmentation and enhanced the performance of skin lesion classification algorithms; Jin *et al.* [7] utilized the neglected knowledge to propose

The associate editor coordinating the review of this manuscript and approving it for publication was Sabah Mohammed .

a cascade knowledge diffusion network for accurate skin cancer classification task; Ghalejoogh *et al.* [8] proposed an optimized neural and fuzzy approach for skin cancer classification.

Notwithstanding automated skin lesion recognition achieves performable diagnosis, it requires large amounts of annotated data from specific scenario, which indicates it is unable to correctly recognize skin cancer on another scenario due to the large distribution-gap between them. This disadvantage severely limits the scalability of automated skin cancer diagnosis models. Here, domain adaptation provides an efficient solution to overcome this limitation, such as Li *et al.* [9] transferred knowledge from a well-labeled source domain to an unlabeled target domain by proposing adversarial tight match method and another method [10] jointly exploited feature adaptation with distribution matching and sample adaptation with landmark selection. To strengthen the adaptive capability of diagnosing models, some attempts firstly introduce domain adaptation into bridging distribution-gap among different skin disease datasets [11]–[14]. They simply pre-train a classification model on another skin disease dataset and fine-tune it on the target data. But an effective domain adaptation method should further distill useful knowledge from the source domain and transfer the information into target domain. Thus, these existing works [11]–[14] only reached poor performance compared to completely supervised skin cancer recognition models. The main reason of this phenomenon is that they adopt universal source data into domain adaptation by global feature learning. However, each source sample contains unique relationship to target, and different views of each skin image express various identical information for diagnosis. Therefore, this paper mainly addresses two problems of how to calculate correlations between source samples to target domain and how to extract various information from different views to further develop the cross-domain automated skin lesion recognition task.

The primary motivations and contributions are briefly concluded as follows.

A. MOTIVATION

(1) Existing skin lesion classification methods are either supervised models with poor expansibility to new scenario, or simply conduct transfer learning by distilling knowledge from all source samples. Therefore, they involve many wrong samples, which have extreme large domain gap to target data, into transfer learning step.

(2) Most skin cancer recognition methods only conduct feature learning on original skin images. That makes some specific information from different views (such as morphology, and texture) may be interfered by some noisy characteristics (such as Gaussian noise) in feature learning procedure. These specific information contribute most discriminative features contained important category-cues for the skin cancer recognition task. Thus, the feature extraction should be conducted from various image views.

(3) Compared to supervised models, existing domain adaptation methods for skin lesion classification achieved unsatisfactory recognition accuracy. That motivates us to develop a novel domain adaptation framework named multi-view filtered transfer learning approach with considerable improvements both on scalability and performance.

B. CONTRIBUTION

(1) We propose a Multi-view Filtered Transfer Learning (MFTL) method for cross-domain skin lesion classification to distill valuable source samples into adversarial domain adaptation and learn various informations from different image views. It can strengthen the representation capability for skin lesion images.

(2) This work designs a source-sample-correlation mining algorithm in deep neural network, and it measures the contributions of each source sample to target domain according to Wasserstein distance.

(3) MFTL employs several feature extractors and classifiers for each view of skin images, leveraging view-information according to their contributions to skin lesion classification. Besides, the validating experiments achieve average AUC of 91.8% on ISIC 2017 dataset [15].

II. RELATED WORKS

This section summarizes the researches on automated skin lesion classification proposed in recent years, including supervised and transfer learning models.

A. SUPERVISED METHODS IN SKIN LESION CLASSIFICATION

Several researches about computer vision algorithms attempt to address challenges in skin cancer diagnosis. In early stage, Binder *et al.* [16] developed an artificial neural network (ANN) for classifying benign and cancerous lesions by dermatologic images with 100 images for training and testing, achieving 88% specificity compared with 90% in human diagnosis. Inspired by ANN model, machine learning methods such as support vector machine [17], K-nearest neighbor [18], Naive Bayesian [19] are utilized into computational skin image analysis. The main drawbacks of these methods are causing computational workloads in pre-process, feature and pattern computation.

In recent years, convolutional neural networks play an important role in skin lesion classification [20]–[23]. This innovative application has achieved excellent classification performance over conventional intelligent methods [24]–[26]. Esteva *et al.* [24] demonstrated classification of skin lesions using a single convolutional neural network (CNN), trained end-to-end from images directly, using only pixels and disease labels as inputs, and it achieved performance on identification of the deadliest skin cancer and most common cancers; Gessert *et al.* [25] proposed a patch-based attention architecture that provides global context between small and high-resolution patches with a novel diagnosis guided loss weighting method, outperformed

TABLE 1. The summary of symbols in this paper.

Symbol	Notation
x_i^s	The i -th skin image in source domain.
y_i	The class label of i -th source image.
x_j^t	The j -th skin image in target domain.
S	The annotated source domain.
T	The unlabeled target domain.
N_s	The Number of source images.
N_t	The Number of target images.
$\mathcal{V}_m(\cdot)$	The m -th view-generator.
\mathcal{F}_m	The feature extractor for m -th source view.
\mathcal{F}_m^t	The feature extractor for m -th target view.
\mathcal{C}_m	The classifier for m -th view.
w_m	The view-weight for m -th view.
M	The total number of image views.
\mathcal{D}_m	The discriminator for m -th view.

previous methods and improves the mean sensitivity by 7%; Harangi *et al.* [26] designed a deep convolutional neural network framework to classify dermoscopy images into seven classes, using GoogLeNet Inception-v3 and achieving remarkable improvement of 7%; Hosny *et al.* [23] integrated deep convolutional neural network architectures (Alex-Net, ResNet-101, and GoogLeNet) on augmented region of interest skin images, with 99.29%, 99.15%, and 98.14% for MED-NODE, DermIS & DermQuest, and ISIC 2017 datasets respectively.

B. TRANSFER LEARNING IN SKIN LESION CLASSIFICATION

Even though deep learning achieves considerable improvements for skin lesion classification compared to hand-crafted feature representation, it requires large amounts of annotated data from target application scenarios. That makes challenging obstacles for the model's expansibility and efficiency, because it is necessary to convene professional doctors with costing much time to generate massive annotations. For the sake of relaxing this inconvenience, many exploitations [13], [14], [27]–[30] have been investigated to apply transfer learning into skin lesion classification. Specifically, transfer learning can distill useful knowledge from a source dataset to an unlabeled target domain, which means that it is unnecessary to mark cost-expensive annotations for target data only needing another existing dataset. Kessem *et al.* [27] utilized a pre-trained GoogLeNet to conduct transfer learning on ISIC 2019, and it successfully classified the eight different classes of skin lesions; Hosny *et al.* [28] presented an automatic skin lesion classification system with higher classification accuracy using the theory of transfer learning and the pre-trained deep neural network; Le *et al.* [13] developed a deep learning system that can effectively and automatically classify skin lesions with an end-to-end deep learning process, transfer learning technique, utilizing multiple pre-trained models and novel class-weighted and focal loss, achieved top-1 classification accuracy of 93%; Mahbod *et al.* [14] investigated and

exploited the transfer learning-based skin lesion classification by a fusion approach with three-level ensemble strategy that exploits multiple fine-tuned networks; Alqudah *et al.* [29] employed GoogLeNet and AlexNet with transfer learning and gradient descent adaptive momentum learning rate for classification of skin lesion images; Hosny *et al.* [30] proposed a highly accurate method utilized transfer learning with pre-trained AlexNet, and it achieved 98.70%, 95.60%, 99.27%, and 95.06% for accuracy, sensitivity, specificity, and precision, respectively.

Though several transfer learning-based models have been integrated into skin lesion classification, they are restricted into fine-tuning pre-trained models and applying them into target data. This transfer learning strategy is severely limited in classification performance because they did not involve the correlations between source and target samples, which can be solved by novel transfer learning technologies.

III. OUR PROPOSED MFTL FRAMEWORK

A. PROBLEM DEFINITION

In our Multi-view Filtered Transfer Learning (MFTL) framework for skin lesion classification, there contains two skin image datasets of S and T . In detail, $S = \{x_1^s, \dots, x_i^s, \dots, x_{N_s}^s\}$ is treated as a completely annotated source domain with its annotation set $Y = \{y_1, \dots, y_i, \dots, y_{N_s}\}$; $T = \{x_1^t, \dots, x_j^t, \dots, x_{N_t}^t\}$ denotes the completely unlabeled target dataset. N_s and N_t represent the numbers of source and target skin images, separately. Here, the goal of MFTL is to distill knowledge about skin lesion classification from filtered source samples into the unlabeled target domain. To generate multiple views of each skin image, we employ several view-generators $\mathcal{V} = \{\mathcal{V}_1(\cdot), \dots, \mathcal{V}_m(\cdot), \dots, \mathcal{V}_M(\cdot)\}$ on both of source and target data, and M is the number of skin image views.

In this study, we divide the proposed MFTL framework into multi-view weighing representation and filtered domain adaptation modules to investigate the transfer learning-based skin lesion classification method.

B. MULTI-VIEW WEIGHING REPRESENTATION

This subsection introduces the preliminary feature representation procedure with weighing each view for the final class prediction. MFTL extracts feature representations for each image view by individual Convolutional Neural Network (CNN) and classifies each view through specific classifiers. Given a source skin image x_i^s , its m -th view can be obtained by $\mathcal{V}_m(x_i^s)$. Thus, M views of x_i^s are generated by $\{\mathcal{V}_1(x_i^s), \dots, \mathcal{V}_m(x_i^s), \dots, \mathcal{V}_M(x_i^s)\}$, through the view-generator sequence \mathcal{V} . Corresponding to each view, MFTL designs M CNN feature extractors $\mathcal{F} = \{\mathcal{F}_1(\cdot), \dots, \mathcal{F}_m(\cdot), \dots, \mathcal{F}_M(\cdot)\}$ with capability of learning appearance feature vectors from each view. To achieve the class prediction for skin lesion images, a sequence of classifiers $\mathcal{C} = \{\mathcal{C}_1, \dots, \mathcal{C}_m, \dots, \mathcal{C}_M\}$ are deployed after each feature extractors. Besides, a novel weighing strategy is

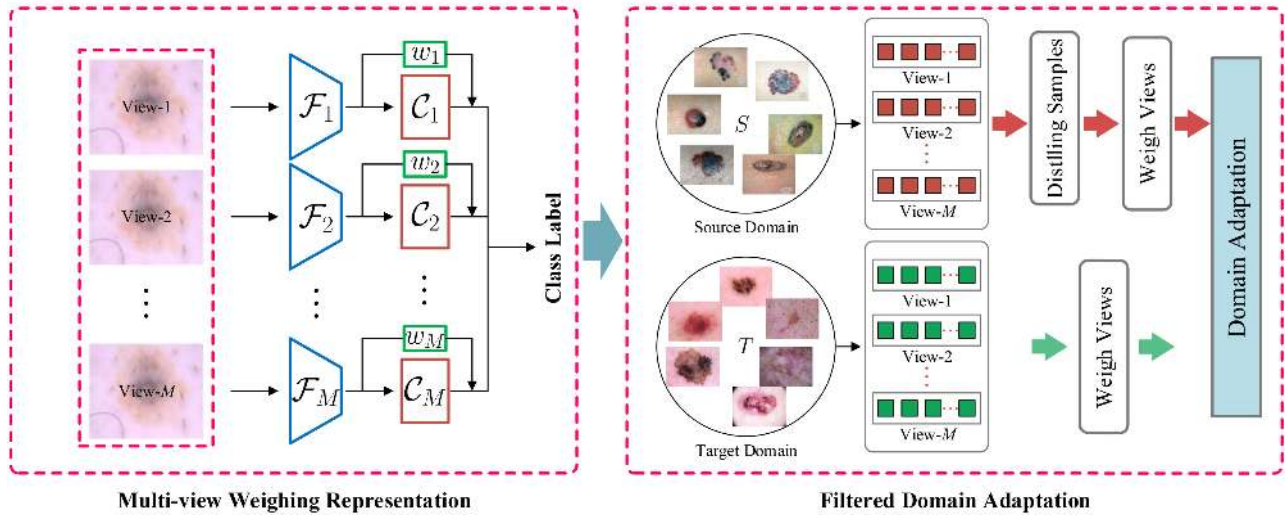


FIGURE 1. The proposed multi-view filtered transfer learning (MFTL) framework. Multi-view weighing representation module contains M CNN feature extractors \mathcal{F}_m and classifiers \mathcal{C}_m , which involve the view-weights w_m into the final prediction; Filtered domain adaptation module chooses useful source samples to transfer valuable knowledge into target domain with the help of source annotations.

integrated after learning CNN feature vectors for each view. This strategy can calculate their weight on the final prediction task.

Mathematically, the feature extractor \mathcal{F}_m and classifier \mathcal{C}_m for m -th view are firstly optimized through cross-entropy loss function,

$$\mathcal{L}_{cls}(\mathcal{F}_m, \mathcal{C}_m) = -\mathbb{E}_{(x_i^s, y_i^s) \in S} \sum_{i=1}^{N_s} y_i \log(\sigma(\mathcal{C}_m(\mathcal{F}_m(\mathcal{V}_m(x_i^s)))))) \quad (1)$$

where σ indicates the softmax function. In contrast to employing a shared CNN feature extractor for learning each view appearance representations, the individual \mathcal{F}_m can exploit more specific characteristics from each view and provide more accurate information for each classifier \mathcal{C}_m .

However, the contributions of each view are different to the skin lesion class prediction task in target domain. Here, we deploy a multi-view weighing component to estimate the importance of each view (2), as shown at the bottom of the next page, where w_m is the weight of m -th view, and m' denotes m' -th view in target domain. Besides, this form of calculation ensures,

$$\sum_{m=1}^M w_m = 1, w_m \geq 0 \quad (3)$$

In the prediction stage, we involve the view-weight into the final classification given a target skin image x_j^t ,

$$\text{Result}(x_j^t) = \sum_{m=1}^M w_m \mathcal{C}_m(\mathcal{F}_m(\mathcal{V}_m(x_j^t))) \quad (4)$$

Here, this prediction function considers more discriminative information from different views of skin image by the estimated view-weights.

C. FILTERED DOMAIN ADAPTATION

1) DOMAIN ADAPTATION

As for the skin images in target domain, a sequence of separate feature extractors $\mathcal{F}^t = \{\mathcal{F}_1^t(\cdot), \dots, \mathcal{F}_m^t(\cdot), \dots, \mathcal{F}_M^t(\cdot)\}$ are deployed to encode target data into source feature space. Here, we employ the adversarial learning strategy to boost target features following source distribution, which is achieved by a group of adversarial discriminators $\mathcal{D} = \{\mathcal{D}_1(\cdot), \dots, \mathcal{D}_m(\cdot), \dots, \mathcal{D}_M(\cdot)\}$. Specifically, the discriminator \mathcal{D}_m and feature extractor \mathcal{F}_m^t for m -th view are optimized adversarially. It maximizes the Wasserstein distance of correctly classified target representations from \mathcal{F}_m^t and the encoded source features from pre-trained \mathcal{F}_m (charged by discriminator \mathcal{D}_m). In detail, \mathcal{F}_m^t attempts to maximize the probability of \mathcal{D}_m making a mistake, that is, minimizing the Wasserstein distance. According to Generative Adversarial Network [31] and Domain Adaptation [32], we assume each discriminator \mathcal{D}_m follows 1-Lipschitz, which is optimized by maximizing the Wasserstein distance,

$$\mathcal{L}_{\mathcal{D}}(\mathcal{D}_m) = \mathbb{E}_{x_i^s \in S} \mathcal{D}_m(\mathcal{F}_m(\mathcal{V}_m(x_i^s))) - \mathbb{E}_{x_t \in T} [\mathcal{D}_m(\mathcal{F}_m^t(\mathcal{V}_m(x_t)))] \quad (5)$$

Meanwhile, \mathcal{F}^t is optimized through minimizing,

$$\mathcal{L}_{\mathcal{F}^t}(\mathcal{F}_m^t) = -\mathbb{E}_{x_t \in T} [\mathcal{D}_m(\mathcal{F}_m^t(\mathcal{V}_m(x_t)))] \quad (6)$$

Following this adversarial training algorithm, the target feature extractor \mathcal{F}_m^t attempts to confuse the discriminator \mathcal{D}_m by minimizing the Wasserstein distance between target image features as the source ones. Besides, a gradient penalty for trainable parameters in each discriminator \mathcal{D}_m is deployed in our method, following [31], [32],

$$\mathcal{L}_{grad}(\mathcal{D}_m) = (\|\nabla_{\hat{\mathbf{F}}_m} \mathcal{D}_m(\hat{\mathbf{F}}_m)\|_2 - 1)^2 \quad (7)$$

where $\hat{\mathbf{F}}_m$ represents the feature collection, containing both of source and target skin image features from \mathcal{F} and \mathcal{F}^t . Here, the discriminator \mathcal{D}_m is jointly trained by minimizing,

$$\mathcal{L}_{\mathcal{D}_m} = -\mathcal{L}_{\mathcal{D}}(\mathcal{D}_m) - \lambda \mathcal{L}_{grad}(\mathcal{D}_m) \quad (8)$$

where λ denotes a balance parameter with pre-defined value.

To train excellent feature encoders \mathcal{F}^t for target domain, we also develop a multi-view adaptation loss inspired by Deep Transfer Metric learning [33],

$$\mathcal{L}_{\mathcal{F}}(\mathcal{F}, \mathcal{F}^t) = \frac{1}{M} \sum_{m=1}^M \left\| \frac{1}{N_s} \sum_{i=1}^{N_s} \mathcal{F}_m(\mathcal{V}_m(x_i^s)) - \frac{1}{N_t} \sum_{j=1}^{N_t} \mathcal{F}_m^t(\mathcal{V}_m(x_j^t)) \right\|^2 \quad (9)$$

This multi-view adaptation loss conducts maximum mean discrepancy constraint on each view from skin images, and it simultaneously optimizes the parameters in \mathcal{F}_m and \mathcal{F}_m^t .

2) SOURCE SAMPLES FILTERING

Considering the samples reveal individual correlations to target domain, this paper proposes a source sample distilling strategy to select more valuable source samples, which can provide positive impacts on domain adaptation between source and target domains. According to the definition of Wasserstein distance, the model chooses more relevant samples with closer distance to target domain. It further improves the target prediction task with the help of selected source samples. The multi-view correlation between source sample x_i^s to target domain can be calculated by the following formula,

$$\gamma_i = \frac{1}{M} \sum_{m=1}^M \left\| \mathcal{D}_m(\mathcal{F}_m(\mathcal{V}_m(x_i^s))) - \frac{1}{N_t} \sum_{j=1}^{N_t} \mathcal{D}_m(\mathcal{F}_m(\mathcal{V}_m(x_j^t))) \right\| \quad (10)$$

According to multi-view correlation calculation, γ_i shows its Wasserstein distance to the target domain. If x_i^s has closer distance to target, it will have a smaller value of γ_i . Here, we select half of source images ($\frac{N_s}{2}$) with smaller γ_i , and obtain the filtered source domain $\hat{\mathcal{S}} = \{x_k^s, y_k\}_{k=1}^{\frac{N_s}{2}}$. With the filtered source samples, we develop the optimization of classifiers in every views from Eq. 1 as,

$$\mathcal{L}_{filtered}(\mathcal{C}_m) = -\mathbb{E}_{(x_k^s, y_k) \in \hat{\mathcal{S}}} \sum_{k=1}^{\frac{N_s}{2}} y_k \log(\sigma(\mathcal{C}_m(\mathcal{F}_m(\mathcal{V}_m(x_k^s)))))) \quad (11)$$

Therefore, the final prediction of the given target skin image x_j^t can be obtained by Eq.4, owing to the joint training of above analyzed network architecture and loss functions.

D. EVALUATION

1) DATASETS

We evaluate the proposed MFTL network on a popular skin lesion dataset (ISIC2017) [15] to measure our performance. Otherwise, this paper employs HAM10000 [43]) as source dataset. In detail, **ISIC2017** [15] dataset is released in 2017 International Symposium on Biomedical Imaging with a task of ternary classification for Malignant Melanoma (MM), Seborrheic Keratosis (SK), and Benign Nevi (BN). Specifically, ISIC 2017 challenge for skin lesion classification provides MM with 374 training, 30 validation, and 117 test images, SK with 254, 42, 90 images, and BN with 1372, 78, 393 images. Here, we utilize the 600 testing images to conduct experiments following [14]; HAM10000 [43] is a large collection of multi-source dermatoscopic images of common pigmented skin lesions, released in ISIC 2018 challenge (task 3). It contains 10,015 skin lesion images of 7 different categories including Actinic Keratosis, Basal Cell Carcinoma, Benign Keratosis, Dermatofibroma, Melanocytic nevi, Melanoma, Vascular Skin Lesion. Compared to ISIC 2017 with three categories, HAM10000 have seven skin lesion classes. To keep class consistency in transfer learning between them, we select Melanoma and Basal Cell Carcinoma (equal to Seborrheic Keratosis) images from HAM10000 in our experiments, which plays the role of source domain and ISIC 2017 is the unlabeled target domain. As for data preprocessing, each skin image is reshaped into 224×224 pixels, and training images are augmented by rotating, flipping, and crop operations in model optimization.

2) NETWORK ARCHITECTURE

In experiments, ResNet-50 [34] is employed as the architecture of feature extractors \mathcal{F} and \mathcal{F}^t (before last fully connected layer), and its last fully connected layer with softmax is deployed as the framework of classifiers \mathcal{C} . The networks are firstly pre-trained on source domain and then further trained on the proposed multi-view filtered transfer learning framework, which converges in 25 epochs. As the setting of multi-view, this paper integrates three image views, including raw image view, texture view (LBP algorithm [44]), and shape view (wavelet transformation [45]). Compared to raw image with whole information, the texture-view only contains texture features and shape-view has more concise shape representations.

3) EVALUATION METRICS

To quantitatively evaluate the performance of our proposed MFTL network, this paper adopts the accuracy, sensitivity, specificity, and area under the receiver operating characteristic curve (AUC) as evaluation metrics. These measurements

$$w_m = \frac{\exp(\frac{1}{N_s} \sum_{i=1}^{N_s} \mathcal{F}_m(\mathcal{V}_m(x_i^s)) - \frac{1}{M} \sum_{m'=1}^M \frac{1}{N_t} \sum_{j=1}^{N_t} \mathcal{F}_{m'}(\mathcal{V}_{m'}(x_j^t)))}{\sum_{m=1}^M \exp(\frac{1}{N_s} \sum_{i=1}^{N_s} \mathcal{F}_m(\mathcal{V}_m(x_i^s)) - \frac{1}{M} \sum_{m'=1}^M \frac{1}{N_t} \sum_{j=1}^{N_t} \mathcal{F}_{m'}(\mathcal{V}_{m'}(x_j^t)))} \quad (2)$$

TABLE 2. Results (%) of our MFTL method and related models on skin lesion classification dataset (ISIC 2017). ‘-’ denotes no result reported in original paper, and the number near the method denotes its reference.

Methods	Melanoma Classification				Seborrheic Keratosis Classification				Avg AUC
	AUC	ACC	Sensitivity	Specificity	AUC	ACC	Sensitivity	Specificity	
ResNet50 [34]	85.7	83.8	63.2	88.8	94.8	84.2	86.7	83.7	90.3
RAN50 [35]	84.9	85.0	62.4	90.6	94.2	86.2	87.8	85.9	89.6
SEnet50 [36]	86.1	84.8	62.4	90.3	95.2	86.3	85.6	86.5	90.7
ISIC#1 [37]	86.8	82.8	73.5	85.1	95.3	80.3	97.8	77.3	91.1
ISIC#2 [38]	85.6	82.3	10.3	99.8	<u>96.5</u>	<u>87.5</u>	17.8	99.8	91.1
ISIC#3 [39]	87.4	87.2	54.7	<u>95.0</u>	94.3	89.5	35.6	<u>99.0</u>	90.9
ARLcNN [40]	<u>87.5</u>	<u>85.0</u>	<u>65.8</u>	<u>89.6</u>	95.8	86.8	<u>87.8</u>	86.7	<u>91.7</u>
MCRes [41]	87.4	-	-	-	95.9	-	-	-	<u>91.7</u>
FusingDeep [42]	87.3	-	-	-	95.5	-	-	-	91.4
TransferFusion [14]	89.2	-	-	-	96.6	-	-	-	92.9
MFTL	87.9 ²	86.2 ³	62.4 ⁴	91.9 ³	95.8 ³	88.0 ²	88.9 ²	87.8 ³	91.8 ²

are calculated by,

$$\text{accuracy} = \frac{TP + TN}{TP + FN + TN + FP} \quad (12)$$

$$\text{sensitivity} = \frac{TP}{TP + FN}, \text{ specificity} = \frac{TN}{TN + FP} \quad (13)$$

$$\text{AUC} = \int_0^1 t_{pr}(f_{pr}) df_{pr} = P(X_1 > X_0) \quad (14)$$

where TP , FN , TN and FP denote the number of true positive, false negative, true negative, and false positive, separately, t_{pr} and f_{pr} represent the true positive rate and false positive rate, X_0 and X_1 are the confidence scores for a negative and positive sample, separately. The AUC value shows the probability that a prediction model ranks a randomly chosen positive sample higher than a randomly chosen negative one. Because ISIC 2017 utilized the AUC value as a gold indicator [15], this work also integrates AUC as a major evaluating criterion.

IV. RESULTS

A. COMPARED WITH BASELINES

To demonstrate the superiority of our proposed multi-view filtered transfer learning approach, we adopts three types of methods to compare, including popular networks (ResNet50 [34], RAN50 [35], and SEnet50 [36]), the top three records in ISIC2017 challenge (#1 [37], #2 [38], and #3 [39]), and recently proposed researches on skin lesion classification (ARLcNN [40], MCRes [41], FusingDeep [42], TransferFusion [14]). Here, we briefly introduce recent skin lesion classification methods. ARLcNN [40] proposed an attention residual learning convolutional neural network for dermoscopy images, composing multiple ARL blocks, a global average pooling layer, and a classification layer; MCRes [41] developed a feasible multi-channel-resnet to assemble multiple residual neural networks for skin lesion analysis, pre-treating the training data with different methods; FusingDeep [42] combined intra-architecture and inter-architecture network fusion for skin lesion images, consisting of multiple sets of different CNN architectures

TABLE 3. Confusion matrix for skin cancer classification tasks. MM denotes Melanoma and SK is Seborrheic Keratosis.

True Label	MM Classification		SK Classification	
	Prediction		Prediction	
	Positive	Negative	Positive	Negative
Positive	73	44	80	10
Negative	39	444	62	448

that represent different feature abstraction levels; TransferFusion [14] proposed a novel fusion approach based on a three-level ensemble strategy that exploits multiple fine-tuned networks trained with dermoscopic images at various sizes. Their results of aforementioned methods and our MFTL are summarized in Table 2, and the unreported evaluation metrics in original papers are annotated by ‘-’.

As demonstrated in Table 2, the proposed MFTL method obtains results (AUC, Accuracy, Sensitivity, Specificity) of (87.9, 86.2, 62.4, 91.9)% on Melanoma Classification task and (95.8, 88.0, 88.9, 87.8, 91.8)% for Seborrheic Keratosis classification. The ranks of each metric are marked next to the results. In detail, there are four metrics ranked in the second best results and others are within top four performance. Besides, we also visualize the ROC curve of our approach on two tasks in Figure 2 and 3, which appears satisfactory visualization on both of Melanoma and Seborrheic Keratosis classification tasks. The confusion matrix is also specified in Table 3, where represents MFTL obtains excellent execution on both classification tasks. Here, it is emphasized that our MFTL only utilizes professional annotations from source domain to predict unlabeled target images, which is benefit from transfer learning and it can economize annotating cost in practical new scenario.

1) COMPARING WITH POPULAR NETWORKS

The first comparison is between MFTL and several popular networks (ResNet50, RAN50, and SEnet50), which can be

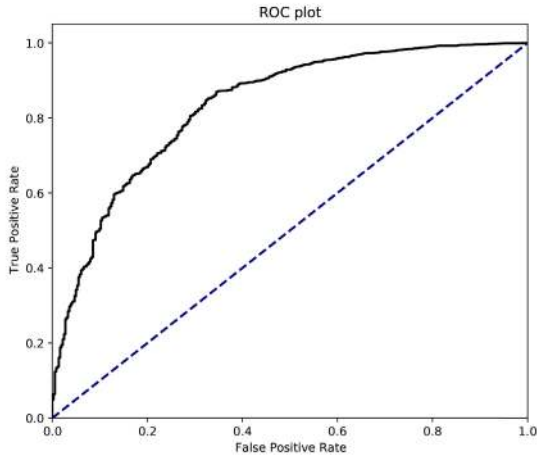


FIGURE 2. Receiver operating characteristic curve of Melanoma classification.

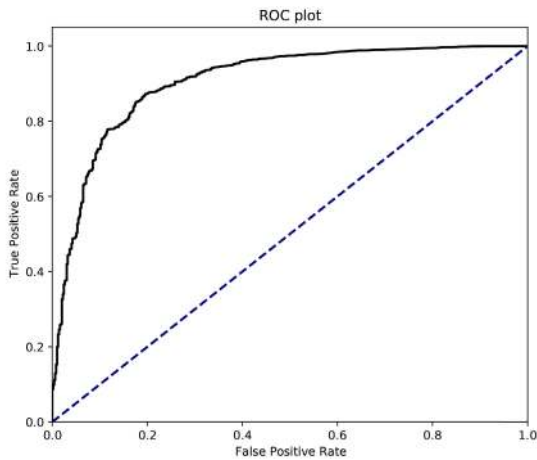


FIGURE 3. Receiver operating characteristic curve of Seborrheic Keratosis classification.

initialized by transferring the pre-trained ResNet50 parameters. As reported in Table 2, the best average AUC among them is achieved by our MFTL with promotion of 1.1%(91.8-90.7)%. These three networks utilize all labels of target dataset, and our method achieves absolute advantages over them. This comparison reveals that our MFTL can not only save the annotating cost, but also perform better results compared to conventional neural networks.

2) COMPARING WITH ISIC CHALLENGE RECORDS

The experimental target dataset is released from 2017 International Symposium on Biomedical Imaging, which is hosted by the International Skin Imaging Collaboration challenge. Here, we select top three records [37]–[39] of ISIC2017 challenge to compare with our method. Especially, Menegola et al. [39] trained the deep neural network with up to

TABLE 4. AUC results of ablation study. MM denotes Melanoma and SK is Seborrheic Keratosis.

Evaluated Module	MM	SK	Avg
Multi-view WR	85.6	91.3	88.5
Single View	86.3	92.9	89.6
Filtered DA	83.2	90.4	86.8
Cosine Similarity in γ_i	86.8	94.0	90.4
MFTL	87.9	95.8	91.8

7500 external images. Different from these records, MFTL only utilizes external data (source) with labels, and transfers knowledge into target domain. Virtually, these works cannot be compared directly with each other due to the differences in training dataset regardless of whether it is an ensemble or not. Nevertheless, these reported results on ISIC 2017 challenge dataset can, to some extent, reflect the state-of-the-art performance in the skin lesion classification task. As shown in Table 2, ISIC #3 achieves the best accuracies both on Melanoma and Seborrheic Keartosis classification tasks; ISIC #2 performs the best specificity on both tasks; and ISIC #1 also obtains the best sensitivity. As for our MFTL, it achieves best AUC, second best accuracy and sensitivity, and third best specificity on Melanoma classification. Besides, it also performs second best AUC, accuracy, and sensitivity on Seborrheic Keratosis classification task. Besides, the average AUC of MFTL is larger than all of these three winners, that reflects our transfer learning strategy contributes a considerable improvement on skin lesion classification task from 2017.

3) COMPARING WITH RECENT WORKS

From ISIC 2017, much research attention [13], [14], [29], [40]–[42] has been paid on skin lesion classification problem. Here, we choose four recently proposed methods [14], [40]–[42] as baselines to validate our performance, with same experiments on the ISIC 2017 dataset. Considering these state-of-the-art methods, our MFTL method achieves the second and third best AUCs on Melanoma and Seborrheic Keratosis classification tasks, separately, while other evaluation metrics also plays satisfactory results over them. This comparison reveals that exploiting transfer learning strategy with multi-view and filtered domain adaptation can further improve the classification performance on skin lesion classification task, while it can save much more professional cost-expensive annotating works in practice.

B. DISCUSSION

The proposed MFTL network contains two major modules of multi-view weighing representation and filtered domain adaptation. Here, we evaluate them to observe their contributions by learning representations from different views, and transferring knowledge from all source samples without any filtering operation. Otherwise, we also evaluate the influence from different distance measurements in Eq.10 to calculate

source-sample-to-target-contribution, and show the convergence of our MFTL model. The evaluated results are reported in Table 4.

1) EVALUATION OF MULTI-VIEW WEIGHING REPRESENTATION

The multi-view weighing representation module considers that different views express more discriminative information from various aspects. Thus, we only learn CNN representations from original image without any other view, which achieves AUC of 85.6% and 91.3% on MM and SK classification tasks. The distances of 2.3(87.9-85.6)% on MM and 4.5(95.8-91.3)% on SK appear the contribution of this module, and it proves that our proposed multi-view weighing representation module plays an important role in our method. Besides, we also evaluate the performance when the proposed method employ single view in addition to utilizing original image. In detail, we iteratively change the adopted single view and calculate the average results as in Table 4. This evaluation improves the average AUC by 1.1(89.6-88.5)% compared to only utilizing original image, while it still expresses a weaker recognizing capability (reducing 2.2% average accuracy) compared to multi-view setting. This modified experiment elaborates that it is a necessary to utilize multiple image views in skin lesion classification task.

2) EVALUATION OF FILTERED DOMAIN ADAPTATION

To evaluate the filtered domain adaptation module, we transfer discriminative ability from all source samples without neglecting any data, which obtains AUCs of 83.2% and 90.4% on MM and SK classification tasks. The considerable improvements of 4.7(87.9-83.2)% and 4.4(95.8-90.4)% on MM and SK classification tasks elaborate that the negative samples has weakened the effectiveness of transfer learning and filtered domain adaptation provides more information than the multi-view weighing representation module.

3) EVALUATION OF DIFFERENT DISTANCE MEASURES IN MULTI-VIEW CORRELATION γ_i

To reveal the influence of different distance measures, which are used to measure the contribution γ_i of each source sample to the target domain in Eq. 10, we integrate Cosine similarity into γ_i , and it obtains 86.8% and 94.0% on Melanoma and Seborrheic Keratosis classification, with reduction of 1.4% in average accuracy. That demonstrates the utilized Euclidean distance is more suitable in the measurement of multi-view correlations among source samples to the target domain, because it is the absolute difference between two high dimensional data but the Cosine similarity is more sensitive to directional data.

4) CONVERGENCE OF MFTL ALGORITHM

To discuss the algorithm convergence of our method, we paint the loss variations along with the training epochs on Melanoma classification experiments. The training and testing losses can be seen in Figure 4, which expresses the

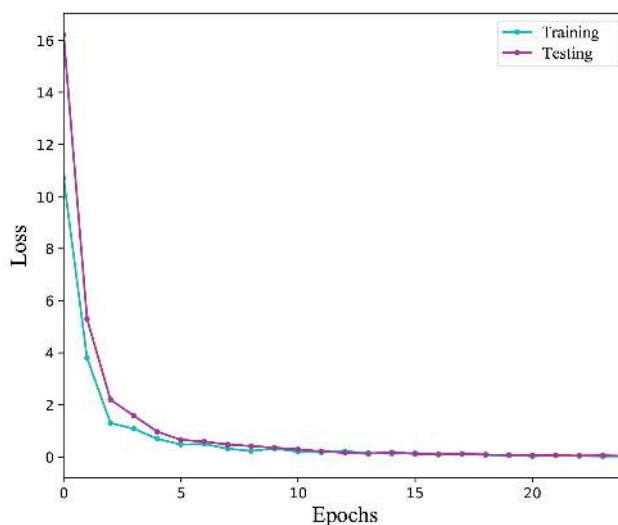


FIGURE 4. Losses of Melanoma classification on training and testing sets.

training converges in 25 epochs and both of training and testing losses are lower than 0.04. Here, this experimental validation proves that our MFTL model can be rapidly converge and optimized within 25 epochs.

V. CONCLUSION

In this study, we attempt to solve the problem that existing skin lesion classification works have poor scalability to new scenario, and several transfer learning researches ignore the negative impact caused from source samples. Thus, we propose a multi-view filtered transfer learning network, which exploits information from different image views by a novel multi-view weighing representation module, and chooses useful source samples without negative effect from source domain by a filtered domain adaptation module. The experimental results of skin lesion classification perform our excellent classification capability on ISIC 2017 dataset with average AUC 91.8% on Melanoma and Seborrheic Keratosis classification tasks. Besides, the evaluation of those two major modules also prove their necessary contributions for our method.

ACKNOWLEDGMENT

(Jianxiao Bian and Shaoqiang Wang contributed equally to this work.)

REFERENCES

- [1] V. Gray-Schopfer, C. Wellbrock, and R. Marais, "Melanoma biology and new targeted therapy," *Nature*, vol. 445, no. 7130, pp. 851–857, 2007.
- [2] H. W. Rogers, M. A. Weinstock, S. R. Feldman, and B. M. Coldiron, "Incidence estimate of nonmelanoma skin cancer (keratinocyte carcinomas) in the US population, 2012," *JAMA Dermatol.*, vol. 151, no. 10, pp. 1081–1086, 2015.
- [3] *Cancer Facts & Figures 2020*, Amer. Cancer Soc., Atlanta, GA, USA, 2020.
- [4] P. Mathur, K. Sathishkumar, M. Chaturvedi, P. Das, K. L. Sudarshan, S. Santhappan, and V. Nallasamy, "Cancer statistics, 2020: Report from national cancer registry programme, India," *JCO Global Oncol.*, vol. 6, pp. 1063–1075, Jul. 2020.

- [5] U. Leiter, U. Keim, and C. Garbe, "Epidemiology of skin cancer: Update 2019," *Adv. Exp. Med. Biol.*, vol. 1268, pp. 123–139, 2020.
- [6] P. M. Pereira, R. Fonseca-Pinto, R. P. Paiva, P. A. Assuncao, L. M. Tavora, L. A. Thomaz, and S. M. Faria, "Skin lesion classification enhancement using border-line features—The melanoma Vs nevus problem," *Biomed. Signal Process. Control*, vol. 57, Mar. 2020, Art. no. 101765.
- [7] Q. Jin, H. Cui, C. Sun, Z. Meng, and R. Su, "Cascade knowledge diffusion network for skin lesion diagnosis and segmentation," *Appl. Soft Comput.*, vol. 99, Feb. 2021, Art. no. 106881.
- [8] G. S. Ghalejoogh, H. M. Kordey, and F. Ebrahimi, "A hierarchical structure based on stacking approach for skin lesion classification," *Expert Syst. Appl.*, vol. 145, May 2020, Art. no. 113127.
- [9] J. Li, E. Chen, Z. Ding, L. Zhu, K. Lu, and H. T. Shen, "Maximum density divergence for domain adaptation," *IEEE Trans. Pattern Anal. Mach. Intell.*, early access, Apr. 28, 2020, doi: 10.1109/TPAMI.2020.2991050.
- [10] J. Li, M. Jing, K. Lu, L. Zhu, and H. T. Shen, "Locality preserving joint transfer for domain adaptation," *IEEE Trans. Image Process.*, vol. 28, no. 12, pp. 6103–6115, Dec. 2019.
- [11] Y. Gu, Z. Ge, C. P. Bonnington, and J. Zhou, "Progressive transfer learning and adversarial domain adaptation for cross-domain skin disease classification," *IEEE J. Biomed. Health Informat.*, vol. 24, no. 5, pp. 1379–1393, May 2020.
- [12] A. Mahbod, G. Schaefer, C. Wang, G. Dorffner, R. Ecker, and I. Ellinger, "Transfer learning using a multi-scale and multi-network ensemble for skin lesion classification," *Comput. Methods Programs Biomed.*, vol. 193, Sep. 2020, Art. no. 105475.
- [13] D. N. T. Le, H. X. Le, L. T. Ngo, and H. T. Ngo, "Transfer learning with class-weighted and focal loss function for automatic skin cancer classification," 2020, *arXiv:2009.05977*. [Online]. Available: <http://arxiv.org/abs/2009.05977>
- [14] A. Mahbod, G. Schaefer, C. Wang, R. Ecker, G. Dorffner, and I. Ellinger, "Investigating and exploiting image resolution for transfer learning-based skin lesion classification," 2020, *arXiv:2006.14715*. [Online]. Available: <http://arxiv.org/abs/2006.14715>
- [15] N. C. F. Codella, D. Gutman, M. E. Celebi, B. Helba, M. A. Marchetti, S. W. Dusza, A. Kallou, K. Liopyris, N. Mishra, H. Kittler, and A. Halpern, "Skin lesion analysis toward melanoma detection: A challenge at the 2017 international symposium on biomedical imaging (ISBI), hosted by the international skin imaging collaboration (ISIC)," in *Proc. IEEE 15th Int. Symp. Biomed. Imag. (ISBI)*, Apr. 2018, pp. 168–172.
- [16] M. Binder, A. Steiner, M. Schwarz, S. Knollmayer, K. Wolff, and H. Pehamberger, "Application of an artificial neural network in epiluminescence microscopy pattern analysis of pigmented skin lesions: A pilot study," *Brit. J. Dermatol.*, vol. 130, no. 4, pp. 460–465, Apr. 1994.
- [17] M. E. Celebi, H. A. Kingravi, B. Uddin, H. Iyatomi, Y. A. Aslandogan, W. V. Stoecker, and R. H. Moss, "A methodological approach to the classification of dermoscopy images," *Computerized Med. Imag. Graph.*, vol. 31, no. 6, pp. 362–373, Sep. 2007.
- [18] K. Ramlakhan and Y. Shang, "A mobile automated skin lesion classification system," in *Proc. IEEE 23rd Int. Conf. Tools with Artif. Intell.*, Nov. 2011, pp. 138–141.
- [19] I. Maglogiannis and C. N. Doukas, "Overview of advanced computer vision systems for skin lesions characterization," *IEEE Trans. Inf. Technol. Biomed.*, vol. 13, no. 5, pp. 721–733, Sep. 2009.
- [20] J. Amin, A. Sharif, N. Gul, M. A. Anjum, M. W. Nisar, F. Azam, and S. A. C. Bukhari, "Integrated design of deep features fusion for localization and classification of skin cancer," *Pattern Recognit. Lett.*, vol. 131, pp. 63–70, Mar. 2020.
- [21] M. Y. Sikkandar, B. A. Alrasheadi, N. Prakash, G. Hemalakhmi, A. Mohanarathinam, and K. Shankar, "Deep learning based an automated skin lesion segmentation and intelligent classification model," *J. Ambient Intell. Humanized Comput.*, vol. 12, pp. 3245–3255, Sep. 2020.
- [22] A. Adegun and S. Viriri, "Deep learning techniques for skin lesion analysis and melanoma cancer detection: A survey of state-of-the-art," *Artif. Intell. Rev.*, vol. 54, pp. 811–841, Jun. 2020.
- [23] K. M. Hosny, M. A. Kassem, and M. M. Fouad, "Skin melanoma classification using ROI and data augmentation with deep convolutional neural networks," *Multimedia Tools Appl.*, vol. 79, nos. 33–34, pp. 24029–24055, Sep. 2020.
- [24] A. Esteva, B. Kuprel, R. A. Novoa, J. Ko, S. M. Swetter, H. M. Blau, and S. Thrun, "Dermatologist-level classification of skin cancer with deep neural networks," *Nature*, vol. 542, no. 7639, pp. 115–118, Feb. 2017.
- [25] N. Gessert, T. Sentker, F. Madesta, R. Schmitz, H. Kniep, I. Baltruschat, R. Werner, and A. Schlaefer, "Skin lesion classification using CNNs with patch-based attention and diagnosis-guided loss weighting," *IEEE Trans. Biomed. Eng.*, vol. 67, no. 2, pp. 495–503, Feb. 2020.
- [26] B. Harangi, A. Baran, and A. Hajdu, "Assisted deep learning framework for multi-class skin lesion classification considering a binary classification support," *Biomed. Signal Process. Control*, vol. 62, Sep. 2020, Art. no. 102041.
- [27] M. A. Kassem, K. M. Hosny, and M. M. Fouad, "Skin lesions classification into eight classes for ISIC 2019 using deep convolutional neural network and transfer learning," *IEEE Access*, vol. 8, pp. 114822–114832, 2020.
- [28] K. M. Hosny, M. A. Kassem, and M. M. Fouad, "Classification of skin lesions using transfer learning and augmentation with alex-net," *PLoS ONE*, vol. 14, no. 5, May 2019, Art. no. e0217293.
- [29] A. M. Alqudah, H. Alquraan, and I. A. Qasmieh, "Segmented and non-segmented skin lesions classification using transfer learning and adaptive moment learning rate technique using pretrained convolutional neural network," *J. Biomimetics, Biomater. Biomed. Eng.*, vol. 42, pp. 67–78, Jul. 2019.
- [30] K. M. Hosny, M. A. Kassem, and M. M. Fouad, "Classification of skin lesions into seven classes using transfer learning with AlexNet," *J. Digit. Imag.*, vol. 33, no. 5, pp. 1325–1334, Oct. 2020.
- [31] I. J. Goodfellow, J. Pouget-Abadie, M. Mirza, B. Xu, D. Warde-Farley, S. Ozair, A. C. Courville, and Y. Bengio, "Generative adversarial nets," in *Proc. Adv. Neural Inf. Process. Syst., Annu. Conf. Neural Inf. Process. Syst.*, Z. Ghahramani, M. Welling, C. Cortes, N. D. Lawrence, and K. Q. Weinberger, Eds. Montreal, QC, Canada: Adv. Neural. Inf. Process. Syst., 2014, pp. 2672–2680. [Online]. Available: <http://papers.nips.cc/paper/5423-generative-adversarial-nets>
- [32] S. Ben-David, J. Blitzer, K. Crammer, A. Kulesza, F. Pereira, and J. W. Vaughan, "A theory of learning from different domains," *Mach. Learn.*, vol. 79, nos. 1–2, pp. 151–175, May 2010, doi: 10.1007/s10994-009-5152-4.
- [33] J. Hu, J. Lu, and Y.-P. Tan, "Deep transfer metric learning," in *Proc. IEEE Conf. Comput. Vis. Pattern Recognit. (CVPR)*, Jun. 2015, pp. 325–333.
- [34] K. He, X. Zhang, S. Ren, and J. Sun, "Deep residual learning for image recognition," in *Proc. IEEE Conf. Comput. Vis. Pattern Recognit. (CVPR)*, Jun. 2016, pp. 770–778.
- [35] F. Wang, M. Jiang, C. Qian, S. Yang, C. Li, H. Zhang, X. Wang, and X. Tang, "Residual attention network for image classification," in *Proc. IEEE Conf. Comput. Vis. Pattern Recognit. (CVPR)*, Jul. 2017, pp. 3156–3164.
- [36] J. Hu, L. Shen, and G. Sun, "Squeeze-and-excitation networks," in *Proc. IEEE/CVF Conf. Comput. Vis. Pattern Recognit.*, Jun. 2018, pp. 7132–7141.
- [37] K. Matsunaga, A. Hamada, A. Minagawa, and H. Koga, "Image classification of melanoma, nevus and seborrheic keratosis by deep neural network ensemble," 2017, *arXiv:1703.03108*. [Online]. Available: <http://arxiv.org/abs/1703.03108>
- [38] I. González Díaz, "Incorporating the knowledge of dermatologists to convolutional neural networks for the diagnosis of skin lesions," 2017, *arXiv:1703.01976*. [Online]. Available: <http://arxiv.org/abs/1703.01976>
- [39] A. Menegola, J. Tavares, M. Fornaciari, L. Tzy Li, S. Avila, and E. Valle, "RECOD titans at ISIC challenge 2017," 2017, *arXiv:1703.04819*. [Online]. Available: <http://arxiv.org/abs/1703.04819>
- [40] J. Zhang, Y. Xie, Y. Xia, and C. Shen, "Attention residual learning for skin lesion classification," *IEEE Trans. Med. Imag.*, vol. 38, no. 9, pp. 2092–2103, Sep. 2019.
- [41] S. Guo and Z. Yang, "Multi-channel-ResNet: An integration framework towards skin lesion analysis," *Informat. Med. Unlocked*, vol. 12, pp. 67–74, 2018.
- [42] A. Mahbod, G. Schaefer, I. Ellinger, R. Ecker, A. Pitiot, and C. Wang, "Fusing fine-tuned deep features for skin lesion classification," *Computerized Med. Imag. Graph.*, vol. 71, pp. 19–29, Jan. 2019.
- [43] P. Tschandl, C. Rosendahl, and H. Kittler, "The HAM10000 dataset, a large collection of multi-source dermatoscopic images of common pigmented skin lesions," *Sci. Data*, vol. 5, no. 1, Dec. 2018, Art. no. 180161.
- [44] T. Ojala, M. Pietikainen, and T. Maenpaa, "Multiresolution gray-scale and rotation invariant texture classification with local binary patterns," *IEEE Trans. Pattern Anal. Mach. Intell.*, vol. 24, no. 7, pp. 971–987, Jul. 2002.
- [45] M. Holschneider, "On the wavelet transformation of fractal objects," *J. Stat. Phys.*, vol. 50, nos. 5–6, pp. 963–993, Mar. 1988.



JIANXIAO BIAN graduated from the Shaanxi University of Science and Technology, in 2014. He is currently pursuing the Ph.D. degree. He is also working with Longdong University, as a Lecturer. His research directions include composite special processing technology and artificial intelligence.



JIANRUI ZHANG received the B.S. and M.S. degrees in mechatronic engineering from Yanshan University, in 2006 and 2009, respectively. He is currently a Ph.D. Scholar with Northwestern Polytechnical University, Xi'an, China. He was a College Lecturer with the College of Mechanical Engineering, Longdong University. He has published one monograph, published more than ten articles, authorized six patents, and six computer software copyrights. He has presided over four research projects. His research interests include mechatronics and robotics.



SONG ZHANG received the bachelor's degree in clinical medicine and the master's degree in pediatrics from Qingdao University, in 2014 and 2017, respectively. She is currently a Pediatric Physician at The Affiliated Hospital of Qingdao University. Her main research areas include blood system diseases and tumors.



SHAOQIANG WANG received the bachelor's degree in network engineering from the Taishan Institute of Science and Technology, Shandong University of Science and Technology, in 2015, and the master's degree in system theory from the Shandong University of Science and Technology, in 2018. He is currently pursuing the Ph.D. degree with the China University of Petroleum (Huadong). He is mainly engaged in artificial intelligence or smart medical research.



JINCHANG GUO graduated from the Lanzhou University of Technology, in 2012, and received the Ph.D. degree. He is currently working with Longdong University, as an Associate Professor. He has participated in the design and manufacture of a number of state-owned large hydropower, thermal power, and nuclear power projects. His research direction includes metal material molding.

...